Investigation of Crystallization of PVCH-PE-PVCH Triblock Copolymer in Supercritical Carbon Dioxide

Pei-Qian Yu,[1] Xu-Ming Xie,[1] Tao Wang,[1] Frank S. Bates[2]

[1]*Advanced Materials Laboratory, Department of Chemical Engineering, Tsinghua University, Beijing 100084, China*
[2]*Department of Chemical Engineering and Materials Science, University of Minnesota, Minneapolis, Minnesota 55455*

ABSTRACT: Crystallization of glassy-crystalline-glassy poly(vinylcyclohexane)-*b*-polyethylene-*b*-poly(vinylcyclohexane) (PVCH-PE-PVCH) triblock copolymer treated in supercritical Carbon Dioxide (scCO$_2$) was investigated by using differential scanning calorimetry (DSC) and atomic force microscope (AFM). It was found that the melting temperatures (T_m) and the crystallinity (X_c) of the PVCH-PE-PVCH samples treated in scCO$_2$ at different annealing temperatures (T) were all much higher than those of the untreated PVCH-PE-PVCH, indicating that the scCO$_2$ could effectively induce the samples to further crystallize. With increasing the T, the T_m of the samples linearly increased, even up to 108°C, close to the T_m ($\sim$ 110°C) of the PE homopolymer hydrogenated from polybutadiene which is equal to the PE block in the

triblock copolymer. The results could be ascribed to the released PE chain ends linked to the PVCH block due to the lowered T_g of the PVCH block swollen by scCO$_2$. It suggested that the origin of the confined crystallization in PVCH-PE-PVCH was the fixed PE chain ends by the glassy PVCH. AFM images of the samples treated in scCO$_2$ showed that the PVCH lamella phase tended to connect each other and led to the aggregated structures. The result indicated that the PVCH block could be availably swollen by scCO$_2$. It supported the DSC experiment results of the samples treated in scCO$_2$. © 2006 Wiley Periodicals, Inc. J Appl Polym Sci 102: 2584–2589, 2006

Key words: PVCH-PE-PVCH; chain ends; confined crystallization; scCO^2; swelling effect

INTRODUCTION

Block copolymers comprise of different sequences (or blocks) that are covalently bound to each other. Usually, block copolymers cause microphase separation due to the chemical incompatibility between the different blocks.[1] As a result, variously ordered thermodynamic equilibrium nanometer length scale structures are formed, such as body-centered cubic spheres, hexagonally packed cylinders, bicontinuous gyroid structure, alternating lamellae, and so on.[1–5]

For glassy-crystalline block copolymers, in general, the minority crystallizable component of block copolymers would have to crystallize within the nanometer length scale structures during cooling from melt, if the T_g of the majority-component was higher than the T_m of the crystallizable component. Some researchers have been paying much attention to this confined crystallization phenomena recently.[2–19] They have investi-

gated the crystallization behaviors and the final morphologies for various block copolymers. It was found that the dramatic changes had taken place in these materials. Generally, the sharply decreased T_m and X_c of the samples were ascribed to the spatial confinement, when the crystallization occurred within the nanometer scale structures.[18] In addition, the crystal nucleation and the growth depended strongly on the type of the microstructures in block copolymers.[5–8]

For some PE-containing glassy-crystalline block copolymers, such as poly (vinylcyclohexane)-*b*-poly (ethylene)-*b*-poly(vinylcyclohexane) (PVCH-PE-PVCH), the PE was prepared by anionic polymerization of poly (1,4-butadiene) (1,4-PB) followed by hydrogenation.[20] The T_m of this PE homopolymer synthesized by the same way was about 110°C due to the $\sim$ 7% ethyl branches in the main chains of the copolymers.[20–22] The structural diagram of PVCH-PE-PVCH triblock copolymer was given in Figure 1.

Several authors[6,21] studied the melt crystallization behaviors of the PVCH-PE-PVCH bulk. During cooling from melt, the crystallization of the PE block usually occurred in microphase-separated structures on account of the high T_g ($\sim$ 140°C) of the PVCH block. Weimann et al.[18] examined the confined crystallization behaviors of PVCH-PE-PVCH triblock copolymer by comparing with PVCH-PE diblock copolymers. The results showed that both the spatial confinement and the fixed chain
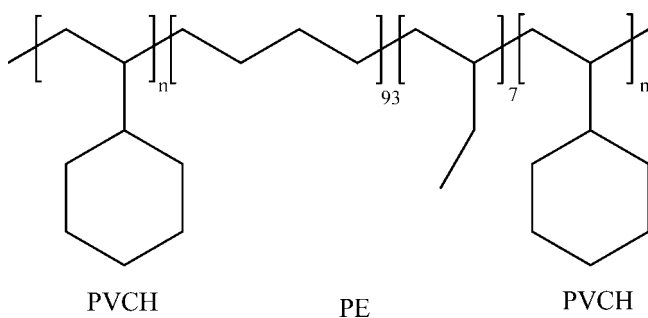
Figure 1 Structural diagram of the PVCH-PE-PVCH triblock copolymer.

ends of PE chain led to the lowered T_m and X_c in the PVCH-PE-PVCH triblock copolymer. However, a detailed discussion on what the main origin of the confined crystallization in this block copolymer is has not been carried out so far.

In our previous paper,[23] the crystallization behaviors of PVCH-PE-PVCH/chloroform solution system were investigated in detail. It was found that the competition between the PE block crystallization and the PVCH block vitrification could be easily controlled through changing the rate of solvent evaporation. If the PE crystallization preceded the PVCH vitrification, the PE block would unrestrictedly crystallize in solution without the confinement of the fixed PE chain ends linked to the PVCH block, leading to the higher T_m. On the other hand, if the PVCH block vitrified first, the glassy PVCH block would fix the chain ends of the PE block. Consequently, the confined crystallization of the PE block resulted in lower T_m, suggesting that the mobility of the PE chain ends linked to the PVCH block strongly affected the PE crystallization in PVCH-PE-PVCH.

Arai et al.[24] and others[25–27] demonstrated that the supercritical carbon dioxide (scCO$_2$) could easily swell amorphous polymer, reduce the interchain interaction, increase the free volume of polymer, lower the T_g of polymer, and improve the mobility of polymer chains. However, the scCO$_2$ had no obvious effect on crystalline polyethylene.[26] So, if the PVCH-PE-PVCH triblock copolymer was immersed in the scCO$_2$, it would be expected that the scCO$_2$ could effectively swell the glassy PVCH block and lower the T_g of the PVCH block in the block copolymer. Therefore, the mobility of the PE chain ends linked to the PVCH block could be improved through changing the glassy state of the PVCH in scCO$_2$, and also the extent of the confinement for the PE crystallization could be changed.

In this paper, the crystallization of PVCH-PE-PVCH triblock copolymers treated in scCO$_2$ is studied. The effect of the PE chain ends on the crystallization of this triblock copolymer will be examined, and the mechanism of the confinement due to the fixed chain ends on the crystallization of the PE block will be elucidated.

EXPERIMENTAL SECTION

Materials and samples preparation

The PVCH-PE-PVCH ($\overline{M}_w = 40,000$; $\overline{M}_w$ (PE) = 16,000; polydispersity index (PDI) <1.10 (Ref. 22); T_g (PVCH) $\sim 140°C$) with the PE weight fraction (w_E) of 0.40 was purchased from Dow Chemical Co.

The PE homopolymer (homo-PE) ($\overline{M}_w = 15,000$; PDI = 2.73, Aldrich), with the weight-average molecular weight almost corresponding to that of the PE block in PVCH-PE-PVCH, was also used. The crystallinity of homo-PE was about 41%, determined by differential scanning calorimetry (DSC), which is comparable to that ($\sim 40\%$) of PE block hydrogenated from PB in our study. Carbon dioxide (CO$_2$) with a purity of 99.95% was purchased from Beijing Analytical Gas Factory. All the polymers and chemicals were used without further purification.

The PVCH-PE-PVCH triblock copolymers were first hot-pressed at 260°C, thus the sheet samples of about 1 mm thickness were obtained. These sheets were then annealed at 220°C for 10 min for getting better microphase separation structure, and then naturally cooled to room temperature. Then the sheets were clamped and put into a stainless steel pressure vessel preheated to a fixed annealing temperature (T). Before pressurized to 20 MPa with CO$_2$, the vessel was flushed thrice with low-pressure CO$_2$. After these sheets were treated in scCO$_2$ for 4 h at different T, the vessel was depressurized and cooled to room temperature naturally. Finally, the sheets were allowed to degas at room temperature for at least 12 h before being used in DSC experiments.

The same process to expose samples to scCO$_2$ at the corresponding T was also performed for the homo-PE.

To examine the effect of the annealing temperature on the crystallization of the samples, both PVCH-PE-PVCH and homo-PE were annealed in the air at different T for 4 h.

For atomic force microscope (AFM) observation, films of about 1 μm thickness were prepared by spin coating from the solution with the concentration of 0.05 g/mL PVCH-PE-PVCH/xylene at 100°C at 1000 rpm on silicon wafers, and then dried at 50°C over 24 h under vacuum. After annealing the films on hot-stage at 160°C for 2 h in the presence of N$_2$, the films were cooled to room temperature naturally. The films were then treated in scCO$_2$. The whole process was similar to the one used for PVCH-PE-PVCH sheet. After the treatment, the surface morphologies of the films were observed by AFM.

Differential scanning calorimetry

The melting temperature (T_m) and the enthalpy of melting (ΔH_m) of each sample were obtained by heat-
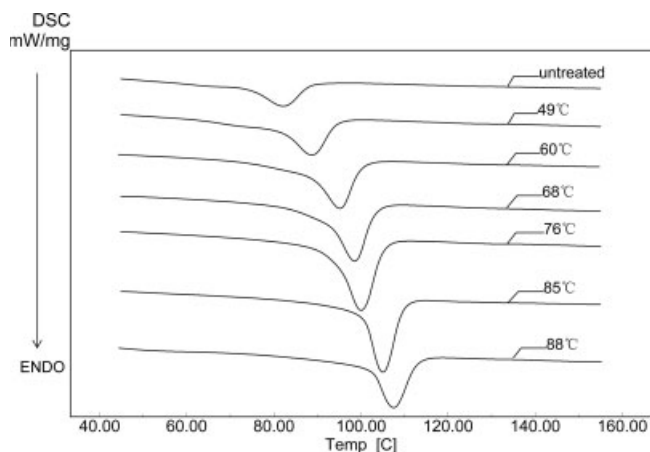
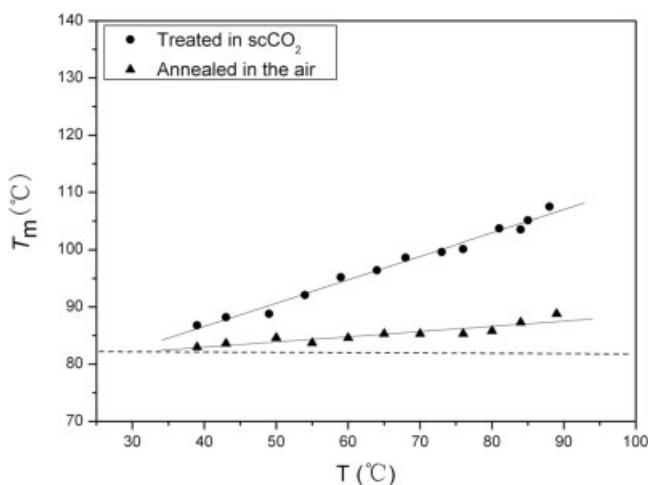**Figure 2** DSC thermograms of the samples untreated and treated in the scCO$_2$ at 20 MPa for 4 h for various T.

ing at a rate of 10°C/min from room temperature to 160°C using a Shimadzu DSC-60 calibrated with indium and Zn. The crystallinity (X_c) of the PVCH-PE-PVCH triblock copolymers was then calculated from ΔH_m by using

$$X_c = \frac{\Delta H_m}{w_E \Delta H_m^0} \qquad (1)$$

where w_E was the weight fraction of PE component in PVCH-PE-PVCH triblock copolymer, ΔH_m^0 was the theoretical heat of fusion of 100% crystalline linear polyethylene (taken as 277.1 J/g).[28]

Atomic force microscopy

AFM images were obtained using a Nanoscope IIIa AFM (Digital Instruments). The AFM was performed under ambient conditions and all images were obtained in tapping mode using commercially available silicon tips. Both topographic and phase images were obtained simultaneously.
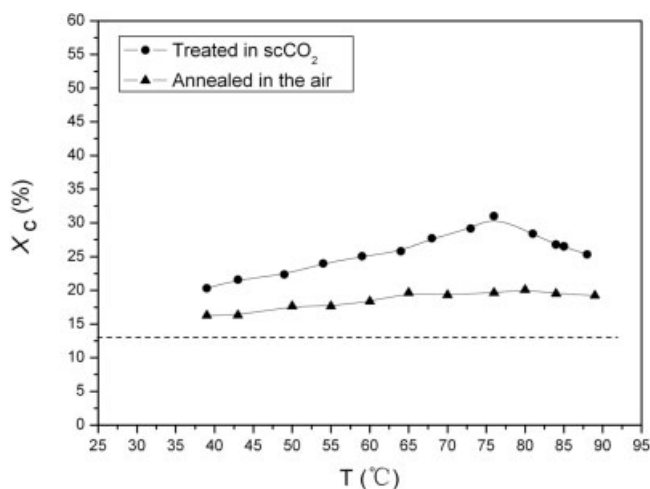
RESULTS AND DISCUSSION

### Changes of the melting temperature and crystallinity

The T_m and X_c of the sheets before and after treatment in scCO$_2$ were examined by DSC. Figure 2 illustrates typical DSC thermograms of the sheets untreated and treated in scCO$_2$ at different T. It is obvious that the melting temperature of the untreated PVCH-PE-PVCH sheet is 82.2°C, which is same as that of the usual confined crystallization samples. With increasing the T, the T_m of the samples treated in scCO$_2$ gradually increases, even up to 108°C as the T reached 88°C, which is close to the T_m ($\sim$ 110°C) of the PE homopolymer hydrogenated from polybutadiene with the $\overline{M}_w$ equal to that of the PE block in the triblock copolymer.[22]

The increase in the T_m of the samples after annealing in scCO$_2$ should be related to the swelling effect of the samples in scCO$_2$ and the effect of the annealing itself.

Figure 3 shows a comparison of the changes in the T_m of the samples treated in scCO$_2$ and annealed in the air at different T. Obviously, either in scCO$_2$ or in the air, the treatments could raise the T_m of all the samples; i.e., both the scCO$_2$ and annealing effect could enhance the crystallization of the PVCH-PE-PVCH. At the same time, both the T_m of the samples treated in scCO$_2$ or annealed in the air seems to linearly increase with increasing the T. It is clear that the increase of the T_m in the samples treated in scCO$_2$ was much larger than that in the samples

Figure 3 Plot of the T_m versus the T for the samples treated in scCO$_2$ and annealed in the air, respectively. The dashed line represents the T_m of the untreated sheet.

Figure 4 Plot of X_c versus the T for the samples treated in scCO$_2$ and annealed in the air, respectively. The dashed line represents the crystallinity of the untreated sheet.
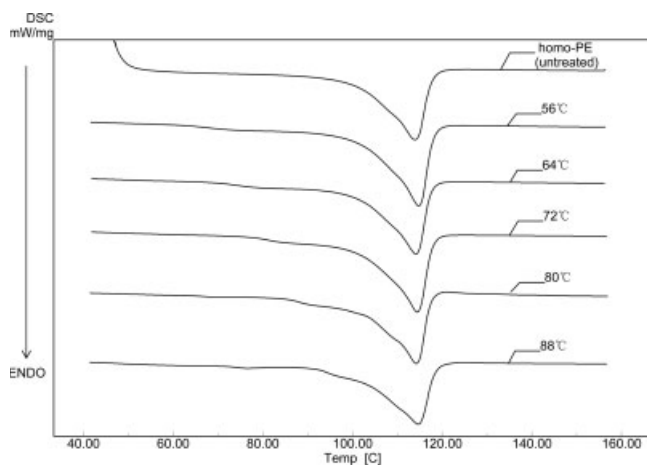
Figure 5 The DSC thermograms of the homo-PE untreated and treated in scCO$_2$ for various T at 20 MPa for 4 h.

annealed in the air. However, the slopes of the two lines are very different, implying that the mechanism of the increase of the T_m in these two cases is different. A similar tendency for the changes in X_c of the samples could also be observed as shown in Figure 4, although X_c of the samples treated in scCO$_2$ slightly decreased when the T was higher than the onset temperature ($\sim$ 75°C) of the melting peak in the DSC curve for the untreated sample. When the annealing temperature is higher than that of the onset, the crystals in the samples must partially melt and induce the decrease in X_c. These results suggested that

the remarkable increases of the T_m and X_c in the samples treated in scCO$_2$ might mostly be ascribed to the effect of the scCO$_2$.

Figure 5 shows the DSC thermograms of the homo-PE untreated and treated in scCO$_2$ at different T. It was evidently that the T_m of all the treated samples was almost as same as the T_m ($\sim$ 114°C) of the untreated homo-PE. Figure 6 shows the plot of X_c versus the T for homo-PE treated in scCO$_2$ and annealed in the air at corresponding temperature for the same time, respectively. The dashed line presents the data of the X_c of untreated homo-PE. It is obvious that the changes of the X_c of homo-PE both treated in scCO$_2$ and annealed in the air were very small and less than 10%. Furthermore, the increment of crystallinity in the samples annealed in the air was larger than that in scCO$_2$. These results revealed that the contribution by the annealing effect to the changes of X_c in homo-PE overwhelmed that by scCO$_2$. These results implied that no effect of scCO$_2$ could be examined on the homo-PE, which is almost corresponding to the PE block in PVCH-PE-PVCH triblock copolymer.

Therefore, we can infer that the scCO$_2$ has no obvious effect on the PE block in the PVCH-PE-PVCH triblock copolymers. However, it is well known that the scCO$_2$ has strong swelling effect on the amorphous polystyrene (PS), resulting in the lowered T_g of the PS.[24,25,27] Because PVCH has similar structure with PS (actually, the PVCH block in the PVCH-PE-PVCH used here was that hydrogenated from PS), it is easily considered that the PVCH block has good
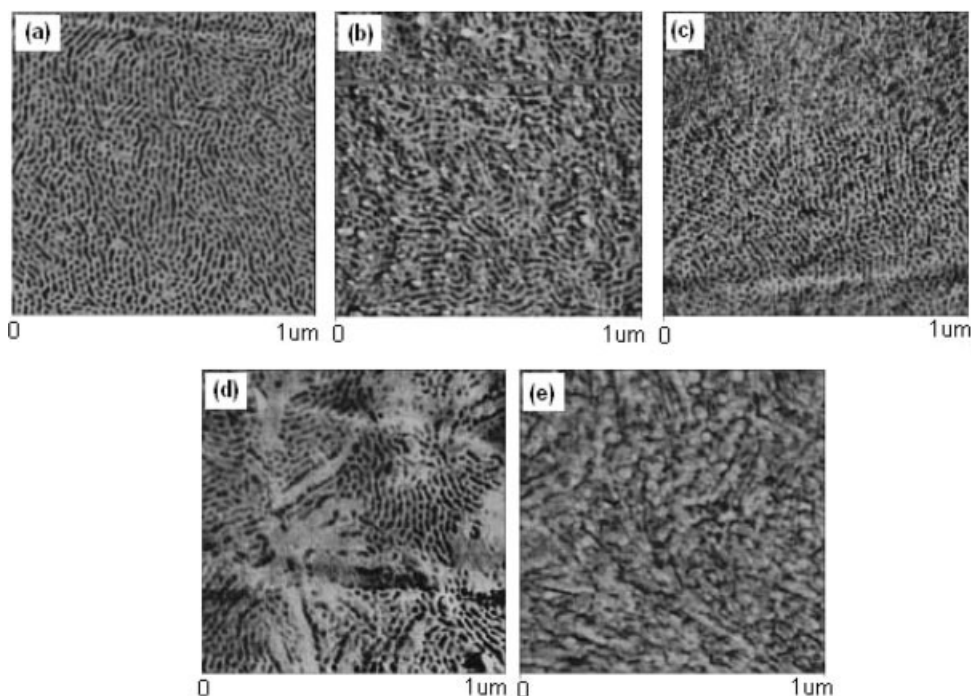
Figure 6 Typical AFM phase images of the spin-coated films untreated (a) and treated in the scCO$_2$ at 20 MPa for 4 h at different T: (b) 49°C, (c) 76°C, (d) 85°C, (e) 88°C.

swelling property and its T_g will be depressed in scCO$_2$ as that of the PS. Once the T_g of the PVCH block was lowered, the fixed PE chain ends linked to the PVCH block in the PVCH-PE-PVCH could be released. It should lead to the improved mobility of the PE chains and the enhanced ability of the crystallization of the PE block. So the remarkable increase in the T_m and X_c of the PVCH-PE-PVCH samples treated in scCO$_2$ as shown in Figures 3 and 4 could be ascribed to the strongly improved mobility of the PE chain ends linked to the PVCH chain due to the lowered T_g of the PVCH block swollen by scCO$_2$.

In conclusion, the confinement of the PE chain ends by the PVCH block in the PVCH-PE-PVCH could be released due to the lowered T_g of the PVCH block swollen in scCO$_2$. These results implied that the confined crystallization in the block copolymers was mainly due to the restricted chain ends of the crystallizable blocks.

Surface morphologies

AFM was used to examine the surface phase structures of the spin-coated films after treatment in scCO$_2$.

Figure 7 illustrates the phase images of the films before and after treatment in scCO$_2$. In these images, the light patterns correspond to the PVCH phases, while the dark patterns correspond to the PE phases, because the Young's modulus of the PVCH phase is larger than that of the PE phase.[22,29] The morphology of untreated PVCH-PE-PVCH ($w_E = 0.40$) formed lamellar microphase separated structures. Similarly, Weimann et al.[18] reported that the PVCH-PE-PVCH triblock copolymer with the PE weight fraction of 0.411 formed lamellar microphase separation structures.

Obviously, the phase structures of the films treated in scCO$_2$ gradually were distorted with increasing the
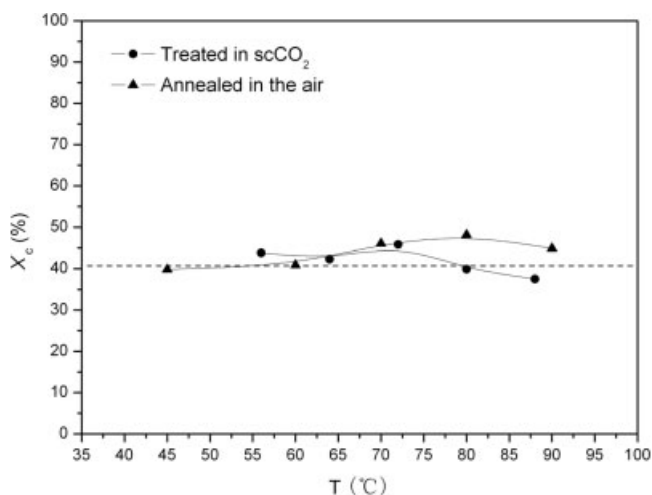
Figure 7 Plot of X_c versus the T for homo-PE after treated in scCO$_2$ and annealed in the air, respectively. The dashed line presents the X_c of the untreated homo-PE.

T. The PVCH lamella phases in the films tended to connect each other and led to the aggregated structures at higher the T. The results indicated that the PVCH block could be availably swollen by scCO$_2$. The higher the T, the easier the scCO$_2$ permeate through the PVCH phase. The permeation of scCO$_2$ led to the lowered T_g of PVCH block. And the PVCH lamella phase should aggregate during the treatment in scCO$_2$, if the T_g of the PVCH is lower than the T. As shown in Figures 7(d and e), it is obvious that the PVCH phase aggregated greatly, and the preexisted microphase-separated structure disappeared at higher the T with the recrystallization of the PE phase. Therefore, the PE chain ends linked to the glassy PVCH block could be released by the swelling effect of scCO$_2$ on the PVCH block during the crystallization of the PE block.

The average dimensions of PE phase (dark phase) was found to be about 13–15 nm by means of section analysis of the images. With scCO$_2$ treatment and annealing, no obvious changes occurred on the sizes of PE phases. It indicated that the changes of T_m and X_c of PE block in PVCH-PE-PVCH triblock copolymer had no direct relationship with the dimensions of PE phase. It is also proved that scCO$_2$ has no obvious effect on PE block. The AFM results support the DSC experiment results of the sheet samples treated in scCO$_2$ as mentioned earlier.

CONCLUSION

The scCO$_2$ could availably permeate through and swell the PVCH block in the glassy-crystalline-glassy PVCH-PE-PVCH triblock copolymers. Consequently, the T_g of the PVCH block was effectively lowered. As the result, the PE chain ends linked to the PVCH block might be released and the mobility of the PE chain ends was greatly enhanced. It led to the remarkable increase in T_m and X_c of the PVCH-PE-PVCH triblock copolymer after the treatment in scCO$_2$, suggesting that the confined crystallization in the PVCH-PE-PVCH triblock copolymer could mainly ascribe to the fixed PE chain ends by the glassy PVCH block.

References

1. Bates, F. S.; Fredrickson, G. H. Annu Rev Phys Chem 1990, 41, 525.
2. Loo, Y.-L.; Register, R. A.; Ryan, A. J. Macromolecules 2002, 35, 2365.
3. Nojima, S.; Kato, K.; Yamamoto, S.; Ashida, T. Macromolecules 1992, 25, 2237.
4. Hamley, I. W.; Fairclough, J. P. A.; Ryan, A. J.; Bates, F. S.; Towns-Andrews, E. Polymer 1996, 37, 4425.
5. Quiram, D. J.; Register, R. A.; Marchand, G. R. Macromolecules 1997, 30, 4551.
6. Loo, Y.-L.; Register, R. A.; Ryan, A. J.; Dee, G. T. Macromolecules 2001, 34, 8968.

7. Hamley, I. W.; Fairclough, J. P. A.; Terrill, N. J.; Ryan, A. J.; Lipic, P. M.; Bates, F. S.; Towns-Andrews, E. Macromolecules 1996, 29, 8835.
8. Hamley, I. W.; Castelletto, V.; Floudas, G.; Schipper, F. Macromolecules 2002, 35, 8839.
9. Opitz, R.; Lambreva, D. M.; de Jeu, W. H. Macromolecules 2002, 35, 6930.
10. Zhu, L.; Chen, Y.; Zhang, A. Q.; Calhoun, B. H.; Chun, M.; Quirk, R. P.; Cheng, S. Z. D. Phys Rev B: Condens Matter 1999, 60, 10022.
11. Zhu, L.; Cheng, S. Z. D.; Calhoun, B. H.; Ge, Q.; Quirk, R. P.; Thomas, E. L.; Hsiao, B. S.; Yeh, F.; Lotz, B. J Am Chem Soc 2000, 122, 5957.
12. Takeshita, H.; Ishii, N.; Araki, C.; Miya, M.; Takenaka, K.; Shiomi, T. J Polym Sci Part B: Polym Phys 2004, 42, 4199.
13. Huang, P.; Zhu, L.; Guo, Y.; Ge, Q.; Jing, A. J.; Chen, W. Y.; Quirk, R. P.; Cheng, S. Z. D.; Thomas, E. L.; Lotz, B.; Hsiao, B. S.; Avila-Orta, C. A.; Sics, I. Macromolecules 2004, 37, 3689.
14. Rangarajan, P.; Register, R. A.; Adamson, D. H.; Fetters, J.; Bras, W.; Naylor, S.; Ryan, A. J. Macromolecules 1995, 28, 1422.
15. Li, L. B.; Yaelle, S.; Michel, H. J. K.; de Jeu, W. H. Macromolecules 2003, 36, 529.
16. Li, L. B.; Lambreva, D.; de Jeu, W. H. J Macromol Sci Phys 2004, 43, 59.
17. Shiomi, T.; Takeshita, H.; Kawaguchi, H.; Nagai, M.; Takenaka, K.; Miya, M. Macromolecules 2002, 35, 8056.
18. Weimann, P. A.; Hajduk, D. A.; Chu, C.; Chaffin, K. A.; Brodil, J. C.; Bates, F. S. J Polym Sci Part B: Polym Phys 1999, 37, 2053.
19. Vittoria, B.; Reimund, S. Macromolecules 1999, 32, 3994.
20. Chen, H.-L.; Hsiao, S.-C.; Lin, T.-L.; Yamauchi, K.; Hasegawa, H.; Hashimoto, T. Macromolecules 2001, 34, 671.
21. Hamley, I. W. Adv Polym Sci 1999, 148, 113.
22. Gehlsen, M. D.; Bates, F. S. Macromolecules 1993, 26, 4122.
23. Yu, P. Q.; Li, H. S.; Wang, Z.; Xie, X. M.; Bates, F. S. Chem J Chin Univ 2005, 26, 583.
24. Arai, Y.; Sako, T.; Takebayashi, Y. Supercritical Fluids, Molecular Interactions, Physical Properties, and New Application; Springer: New York, 2002; p 324.
25. Kiran, E.; Johanna, M. H.; Levelt, S. Supercritical Fluids: Fundamentals for Application; Kluwer Academic: Dordrecht, 1994; p 554.
26. Boyer, S. A. E.; Grolier, J. P. E. Polymer 2005, 46, 3737.
27. Zhang, Z.; Handa, Y. P. Macromolecules 1997, 30, 8505.
28. Brandrup, J.; Immergut, E. H.; Grulke, E. A. Polymer Handbook, 4th ed.; Wiley: New York, 1999; Vol. 13.
29. Sperling, L. H. Introduction to Physical Polymer Science; Wiley: New York, 2001.